Anwar, Ali A. and Ritos, Konstantinos and Gorash, Yevgen and Dempster, William and Nash, David (2016) Microflow leakage through the clearance of a metal-metal seal. In: ASME Pressure Vessels & Piping Conference 2016, 2016-07-17 - 2016-07-21, Hyatt Regency Vancouver. (In Press) ,

This version is available at https://strathprints.strath.ac.uk/57283/

PVP2016-63848

DRAFT: MICROFLOW LEAKAGE THROUGH THE CLEARANCE OF A METAL-METAL SEAL

Ali A. Anwar[*]
WEIR Advanced Research Centre
Mechanical and Aerospace Engineering
University of Strathclyde
Technology and Innovation Centre
99 George St, Glasgow, G1 1RD
ali.anwar@strath.ac.uk

Konstantinos Ritos
Yevgen Gorash
William Dempster
David Nash

Mechanical and Aerospace Engineering
University of Strathclyde,
James Weir Building
75 Montrose St, Glasgow, G1 1XJ
konstantinos.ritos@strath.ac.uk,
yevgen.gorash@strath.ac.uk,
william.dempster@strath.ac.uk
d.nash@strath.ac.uk

ABSTRACT

The motivation behind this study is to simulate high pressure gas flow through the clearance between a valve seat and disc when in a closed position using a representative model. This leakage phenomenon is common in metal-to-metal seal pressure relief valves. As a pressure relief valve reaches the set pressure, it is known for the leakage to increase. The representative model that we studied is of an ideal-gas flow through a 2D microchannel in the slip flow regime. We used a laminar continuum flow solver which solved the mass, momentum and energy equations. In addition, we applied low pressure slip boundary conditions at the wall boundaries which considered Maxwells model for slip. The channel height was varied from 1µm to 5µm while the length remained at 1.25 mm, this means the length to height ratio varied from 1250 to 250. Inlet pressure was varied from a low pressure (0.05 MPa) to a high pressure (18.6 MPa), while the outlet remained constant at atmospheric. The calculated mass flow rate is compared to an analytical solution giving very good agreement for low pressure ratios and high length to height ratios.

NOMENCLATURE

h	channel height
k	Boltzmann's constant
L	channel length
m	molecular mass
$\dot{m}$	mass flow rate
R	gas constant
T	temperature
x	position along length of channel

Kn_1	Knudsen Number at exit
P_0	Pressure at inlet
P_1	Pressure at exit
μ	viscosity
σ	accommodation coefficient

INTRODUCTION

Pressure Relief Valve (PRV) leak tightness guarantee provided by manufacturers is of great importance to both consumers and manufacturers. A consumer would want to ensure the leak tightness is guaranteed to safeguard working conditions. To guarantee the leak tightness, a PRV must comply with standards such as API 527: Seat Tightness of Pressure Relief Valves [1] and

---

[*]Address all correspondence to this author.

dependant on region the equivalent standard would be used i.e. British Standard-BS EN ISO 4126-1:2013 [2]; ASME Standard-ASME PTC 25-2014 [3], etc. As a PRV reaches its set pressure the leakage rate increases. Therefore having the ability to design according to standards and reduce the leakage of a PRV allows valve manufacturers to create market competitive products.

Primarily, this paper aims to allow designers of PRV's to consider fluid flow through a channel created between the valve seat and disc. The channel considered in this study is represented as a microchannel, while the fluid flow conditions are in the regime of slip flow. Due to the nature of the problem, the findings in this study and modelling approach can be extended for other geometric models to account for other devices or high pressure fields such as pipe sealing or gaskets.

The channel is modelled as 2D (as shown in Figure 1) being representative of a PRV seat and disc contact length (L). The channel (or gap) can be attributed to an average spacing between the seat and disc contacting surfaces with respect to surface roughness, waviness and/or form i.e. the finish quality of the metal-to-metal contacting surfaces [4].

The first analysis in this study focuses on the effects of changing the inlet pressure, P_0, from 1 MPa to 18.6 MPa over a fixed channel height (h) of 1μm and length of 1.25 mm (L/h=1250) using CFD. For this study the internal pressure is higher than the external pressure, P_1 (remaining at atmospheric), consequently driving the gas to the outer extremity of the seat and disc length. This allows examination of the pressure profile across the '*Pressure Profile Line*' (see Figure 1) which is the midline between seat/disc contact and how well it fairs with analytical equations. The channel height is then changed to 5μm (L/h=250) and the mass flow rate is analysed.

The second analysis focuses on varying the channel ratio, L/h, from 1250 to 250 for the highest pressure of 18.6 MPa and seeing how this effects the mass flow rate. This is to distinguish at which point the analytical equations are no longer appropriate.

The pressure distribution across the seat/disc length and the mass flow rate is calculated using the CFD solver, ANSYS Fluent v16.1 and compared against analytical models. The analytical models used were formulated by the well known equations/formula of Arkilic et al [5] that takes into account rarefraction in calculating the pressure distibution and mass flow rate at the exit across a parallel channel. A more recent analytical equation by Chong [6] for chocked flow is also compared and assessed.

Background

Arkilic et al's [5] analytical Eqn. (1) of the modified Navier-Stokes equation has shown good agreement with the classical microchannel pressure profile experiment conducted by Pong et al [7]. Arkilic et al's own experimental work showed good agreement with Eqn. (1).
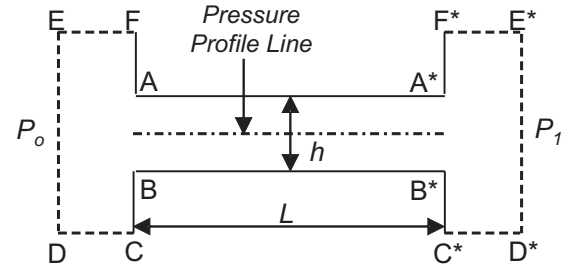

FIGURE 1. Sketch of computational regions

$$\frac{P(x)}{P_1} = \left\{ a^2 - b\left(\frac{x}{L}\right) \right\}^{\frac{1}{2}} - 6Kn_2$$

$$where; \quad a = \left(6\text{Kn}_2 + \frac{P_0}{P_1} \right)$$

$$b = \left[\left(\frac{P_0^2}{P_1^2} - 1 \right) + 12\text{Kn}_2 \left(\frac{P_0}{P_1} - 1 \right) \right]$$

(1)

Other authors have also shown good agreement with Eqn. (1) and Pong et al's experiment by conducting similar studies using up to pressure ratios (P_0/P_1) of 3.95 (as shown in Table 1) for subsonic flows.

In past work, the channel length and height ratio (and Knudsen number) is such that the $L/h >1000$. This means that the poiseuille flow equation is satisfied since it is assumed that the $L/h \gg 1$ and, low Mach numbers, isothermal flow is considered between two parallel plates [8]. Using Arkilic et al's [5] equation the mass flow rate can be calculated (which accounts for rarefaction) using:

$$\dot{m} = \frac{h^3 P_0^2}{24\mu RT} \left[P_0^2 - P_1^2 + 12\frac{2-\sigma}{\sigma} Kn_1 P_1 (P_0 - P_1) \right]$$

(2)

Equation 2 has however been used for $L/h <1000$ by Chong, who considers chocked conditions for subsonic flow. Chong accounts for subsonic flow conditions using the equation below:

$$\dot{m} = \frac{h^3 P_0^2}{24\mu RT} \left(1 + 12\frac{(2-\mu)}{\mu} \frac{\sigma}{P_1 h} \frac{16}{5} \sqrt{\frac{kT}{2\pi m}} \right).$$

(3)

Chong creates this equation by assuming the pressure ratio (P_0/P_1) tends to infinity for subsonic chocked flow conditions in the microchannel. This analytical equation is also compared in this study, however what stands out is that there are no terms to consider the effects of compressibility i.e. the change in density/temperature as the transition is made from subsonic to chocked conditions. This is discussed latter.

. Selected authors who have conducted experiments and compared Eqn. (1) and Eqn. (2) for various pressure ratios (P_0/P_1) and L/h conditions.

Research Papers	L/h	P_0/P_1	Kn
Pong et Al (1994) [7]	2500	1.35-2.75	Slip Flow
Arkilic et Al (1997) [5]	>5600	1.2-2.5	Slip Flow
Zohar (2002) [9]	≥4000	2.5-3.95	Slip Flow
Chong (2006) [6]	5-100	1-32	Slip Flow–Continuum

SIMULATION CONDITIONS AND METHOD

Figure 1 shows the 2D sketch of the simulated microchannel with channel size, h, spanning from AB to A*B* with a fixed length, L=1.25 mm. AB is the inlet and A*B* is the outlet of the microchannel. A buffer region is added either side of the inlet and outlet of the microchannel (zone CDEF and C*D*E*F* respectively). If the buffer regions were not present then it would mean analysing results at the boundary condition of the inlet and the outlet, with no guarantee of the model flow being fully developed at those points.

For the CFD simulations, it is assumed that the temperature at the walls and of the laminar flow of gas is 295K and the fluid is an ideal gas being air. The walls AA* and BB* have also a low pressure boundary slip condition applied which allows the Maxwells model for velocity slip and temperature change to be considered ($0.01< Kn <0.1$) [10].

The CFD simulations have been conducted in ANSYS Fluent v16.1 for these studies. A meshing example of the inner buffer region for channel height of 1 μm is shown in Figure 2. As shown, the meshing becomes more concentrated as we travel towards the inlet of the microchannel. Similarly the walls AB and A*B* have many layers/divisions with a bias towards the wall. This allows the velocity and temperature change across the wall to be captured with better precision.

The first results focus on a channel height of 1 μm (L/h=1250) with the pressure inlet varied from 1-18.6MPa. Specifically, pressure inlet (P_0) values of 1, 5, 10, 15 and 18.6MPa are analysed. After which the mass flow rate is found at the outlet, A*B*, for a channel height of 1 μm and 5 μm (L/h=250). The CFD simulation is compared agaisnt Eqn. 1 to see how well the analytical model fairs against the CFD. Similarly the mass flow rate calculated via the CFD is compared to Eqn. 2 and Eqn. 3.

The second set of results focus on changing the L/h ratio from 1250-250, specifically L/h values of 1250, 1136, 1042, 961.5, 892.9, 833.3, 625, 416.7, 312.5 and 250 and measuring the mass flow rate. This time the focus is primarily on seeing the difference between the analytical Eqn. 2 and the CFD calculations.
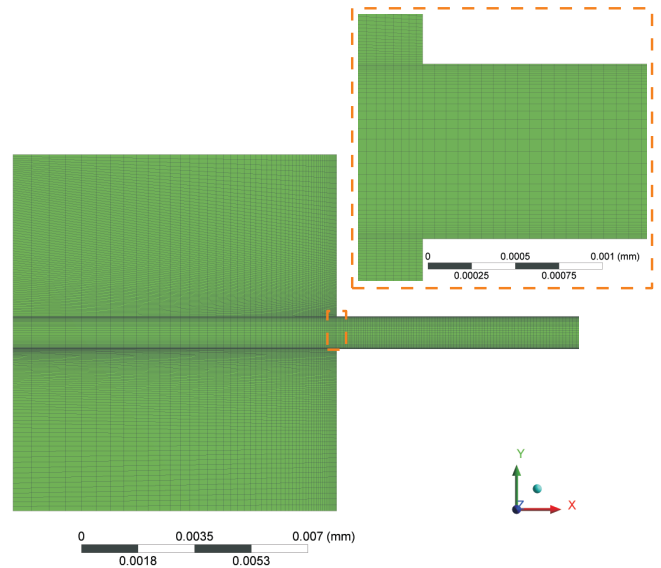

FIGURE 2. Mesh of inner buffer region where h=1μm

RESULTS AND ANALYSIS

The first set of results shown in Figure 3 are of the pressure profile across the seat length, L.

As it can be be seen there is good agreement when P_0 up to 5 MPa (P_0/P_1=49.3) between the CFD simulation and the analytical model. There is a very slight deviation between the 5 MPa which begins at about 0.88 mm along the channel length. Referring to Figure 4, this is most likely because the Mach number at the exit reaches 1 for this condition meaning that compressibility effects on the gas need to be considered. This measurement is however taken at the centreline of the channel (*Pressure Profile Line*). As we move toward either wall of the channel the Mach number decreases.

As the inlet pressure is ramped up to 18.6 MPa the deviation between the analytical Eqn. (1) and simulated results becomes more prevalent for each pressure increment. Only the final 2 μm of the channel length show chocking conditions. This is due to the compressibility of the gas becoming more apparent and not being considered in the analytical model. Equation 1 was originally formulated for Micro-Electro-Mechanical Systems (MEMS) equipment [8] which require low pressure ratios, sub-sonic flow conditions, therefore this deviation between the CFD and analytical results for $P_0/P_1 \geq$49.3 is not surprising.

The next set of results of interest are of the mass flow rate at the exit of the microchannel. It is with the mass flow rate we can attribute leakage. So, for $h = 1\mu$m (L/h=1250) and $h = 5\mu$m (L/h=250) the mass flow rate is calculated using Eqn. (2) and Eqn. (3) and comparing it against the CFD simulation for the same pressure range as before. The results are shown in Figure 5 and Figure 6.

It can be seen for the L/h=1250, the mass flow rate for the CFD simulation and the analytical equations compare well. While for the L/h=250 it is clear that after 5 MPa the analytical equations tend toward an exponential direction. While the CFD
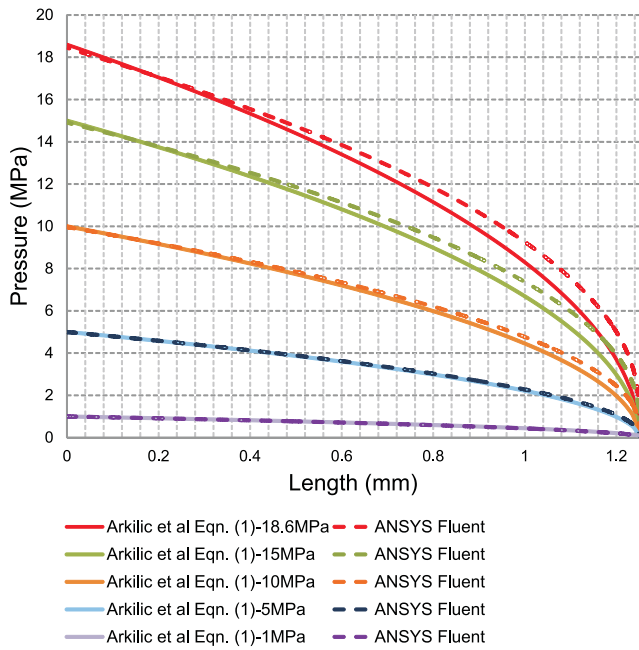
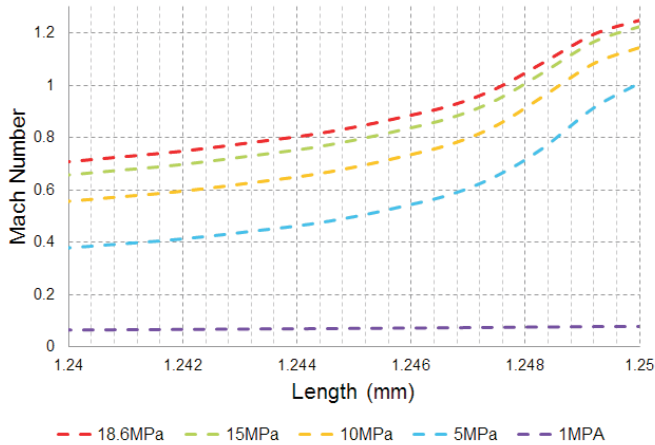**FIGURE 3.** Graph of Pressure profile versus length for h=1μm

FIGURE 4. Mach Number versus channel length (last 0.1mm) for h=1μm

solver follows a straight line trend.

Equation 3 shows negligible difference in comparison with Arkilic et al's Eqn. (2). As discussed earlier, it is known that at 5MPa the Mach number was found to be 1 at the exit, therefore the percentage difference found at 5MPa is 51% between Eqn. 3 and the CFD simulation. Chong [6] has stated to find a difference of 45% between the DMCS and Eqn.(3) for a Mach number of 0.9 at the exit due to a pressure ratio of 32. Therefore, there is good correlation here between Chong's study and this CFD study. It should be noted that Chong used a much lower L/h ratio of 5. It would be worthwhile to simulate the exact same experiment conducted by Chong and compare it using CFD to see how well CFD fairs with the Direct Simulation Monte Carlo
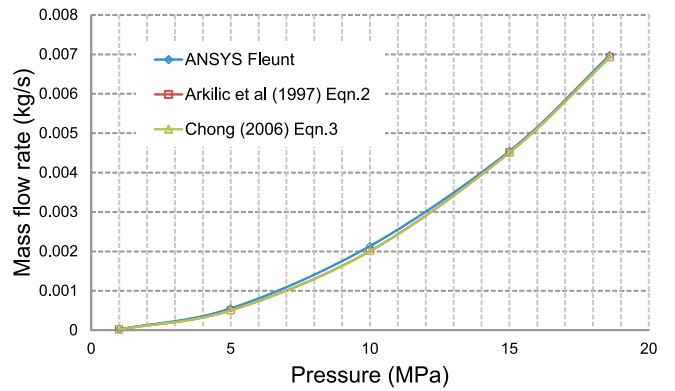

FIGURE 5. Graph showing the effect of P_0 change from 1MPa-18.6MPa versus the mass flow rate for a channel of h=1 μm
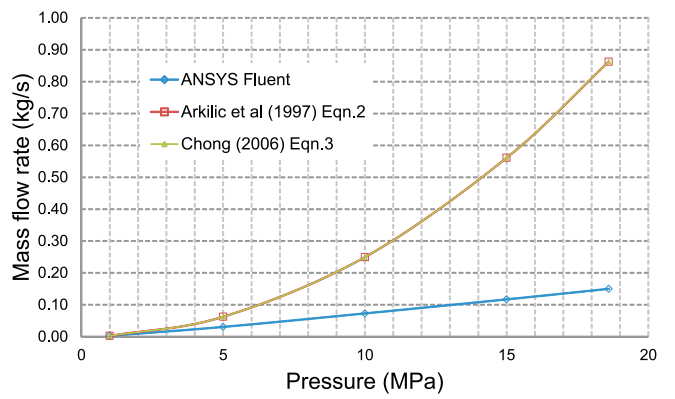

FIGURE 6. Graph showing the effect of P_0 change from 1 MPa-18.6 MPa versus the mass flow rate for a channel of h=5 μm

(DSMC) method for Chong's scenario.

However, this good correlation does not detract from the exponential difference between the CFD simulation and the analytical equations as seen in Figure 6. As stated earlier Eqn.(2) created by Arkilic et al is only applicable for subsonic flows and therefore does not consider the effects of compressibility. Also it is based on Poisellue flow which assumes that $L/h >$1000. To analyse the effects of L/h the previous analysis is extended to find the mass flow rate for a inlet pressure of 18.6 MPa for L/h ratios of 1250, 1136, 1042, 961.5, 892.9, 833.3, 625, 416.7, 312.5 and 250. The results are plotted in Figure 7.

Up to a L/h ratio of 1000 there is a maximum difference of 16% between the CFD and analytical model. When $L/h >$1000 there is another exponential increase in the difference between the CFD and analytical calculations increasing all the way up to 475%. This shows that the compressibility effects of the gas are likely to be a much more dominating effect. To conclusively know if the CFD solver is correctly calculating the pressure profile and mass flow rate, experiments would be required, replicating the a $L/h <$1000 and high pressure ratios which are capable of chocked flow conditions. Also the DSMC method should
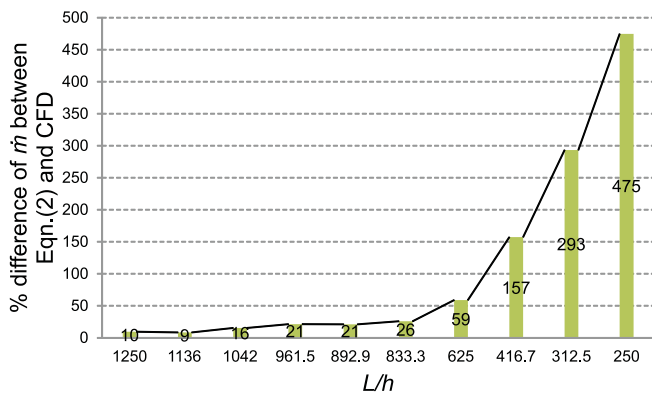
4

FIGURE 7. Graph showing the effect of changing L/h from 1250-250 versus the percentage difference of the mass flow rate between the Arkilic et al analytical Eqn. (2) and the CFD solver (ANSYS)

be ran in parallel similar to Chong's analysis method (excluding Eqn. 3).

CONCLUSIONS

This study has shown that for low pressure ratios of $P_0/P_1 < 49.3$ where the flow conditions are not able/capable to create chocked flow conditions in a microchannel and with a $L/h > 1000$, the analytical equations created by Arkillic are appropriate since they disregard the effect of compressibility.

However, for high pressure ratios of $P_0/P_1 \geq 9.87$ where the flow conditions create a chocked flow in a microchannel and with a $L/h < 1000$, the analytical equations created by Arkillic and Chong are not appropriate since they disregard the effect of gas compressibility. Instead CFD and DSMC simulations for this condition are likely to be of greater reliance since they do take into consideration the effects of compressibility of the gas as it reaches the outlet of the microchannel. Experimental studies would be required to validate the CFD and DSMC simulations.

ACKNOWLEDGMENT

REFERENCES

[1] API, 2014. *Seat Tightness of Pressure Relief Valves*. No. 527 in API Standard. American Petroleum Institute, Washington, USA.

[2] BSI, 2013. *Safety devices for protection against excessive pressure. Safety valves*. No. BS EN ISO 4126-1:2013 in British Standard. The British Standards Institution, London, UK.

[3] ASME, 2014. *Pressure Relief Devices – Performance Test Codes*. No. ASME PTC 25-2014 in An American National Standard. The American Society of Mechanical Engineers, New York, USA.

[4] Anwar, A., Gorash, Y., Dempster, W., and Hamilton, R., 2015. "Literature research in relevant fields to understand pressure relief valve leak tightness in a static closed state". *Procedia Engineering, 130*, pp. 95 – 103.

[5] Arkilic, E. B., Schmidt, M., Breuer, K. S., et al., 1997. "Gaseous slip flow in long microchannels". *J. of Microelectromechanical Systems, 6*(2), pp. 167–178.

[6] Chong, X., 2006. "Subsonic choked flow in the microchannel". *Physics of Fluids, 18*(12), pp. 127104–1–127104–5.

[7] Pong, K.-C., Ho, C.-M., Liu, J., and Tai, Y.-C., 1994. "Non-linear pressure distribution in uniform microchannels". *ASME-PUBLICATIONS-FED, 197*, pp. 51–51.

[8] Karniadakis, G. E., Beskok, A., and Aluru, N., 2006. *Microflows and nanoflows: fundamentals and simulation*, Vol. 29. Springer Science & Business Media.

[9] Zohar, Y., Lee, S. Y. K., Lee, W. Y., Jiang, L., and Tong, P., 2002. "Subsonic gas flow in a straight and uniform microchannel". *Journal of fluid mechanics, 472*, pp. 125–151.

[10] ANSYS® Help, 2015. *Fluent // Theory Guide // 7. Species Transport and Finite-Rate Chemistry // 7.2.3. Slip Boundary Formulation for Low-Pressure Gas Systems*, Academic Research 16.1.0 ed. ANSYS, Inc., Canonsburg (PA), USA.